

Washout of Cr(III)-Acetate-HPAM Gels From Fractures: Effect of Gel State During Placement

B. Brattekås, S. G. Pedersen, H. T. Nistov, Å. Haugen, and A. Graue, University of Bergen; J. -T. Liang, University of Kansas; and R. S. Seright, New Mexico Petroleum Recovery Research Center

Summary

This work investigated the blockage performance of a Cr(III)-acetate-hydrolyzed polyacrylamide (HPAM) gel after placement in open fractures, with emphasis on the effect of gel maturity during placement. Polymer gel is formed through a chemical reaction between a polymer and a crosslinking agent (in a gelant solution) that occurs during the gelation time. In field applications, gelant is generally pumped from the surface, but gelation may occur during injection because of high-temperature conditions and longer pumping times; hence, partially or fully mature gel may exit the wellbore during polymer-gel injection in a fractured reservoir. Gelation alters the solution properties significantly; hence, immature gelant and fully formed (mature) polymer gel show different behavior during placement in a fractured system, and the gels deposit differently in the fracture volume. Injection of gel at different maturities in a fracture may therefore influence the ability of the gel treatment to block fractures, and hence its performance during conformance-control operations. Placement of immature and mature gels and their ability to block fractures during subsequent waterfloods were investigated in this work.

Gel was placed in fractures (and in the surrounding core matrix for some application regimes) in its immature (gelant) or mature state. The gel-blockage performance was assessed by recording gel-rupture pressures and subsequent residual resistance factors during chase waterfloods. Placement of mature gel in open fractures yielded consistent rupture pressures during subsequent water injections, following linear trends for given gel-placement rates and throughput volumes. The rupture pressures were predictable and stable in all the core materials studied. Rupture pressures achieved after placement and in-situ crosslinking of immature gel (gelant) were comparable with rupture pressures achieved after mature-gel placement, but were less predictable. Placing immature gel in the adjacent matrix and in the fracture increased the resistance to gel rupture compared with placing gel in the fracture volume only. In some cores, gel did not form after placement in its immature state. Interactions between Bentheim rock material and gelant were observed, and believed to be the primary cause for lack of gelation.

Significant permeability reduction was achieved during subsequent waterfloods after placement of either immature or mature gel in open fractures. Residual resistance factors for cores treated with gel and gelant were comparable initially. After significant water throughput, substantially greater pressure gradients were observed in cores treated with formed gel rather than gelant crosslinked in situ, and the permeability reduction averaged 5,000 for mature gel and 600 for gelant-treated cores.

Introduction

High permeability contrasts in fractured reservoirs may cause channeling of injected fluids through fracture networks, contributing to

low sweep efficiency and an increased waste stream from excess production of water. The production oil cut may be increased by reducing fracture conductivity (Graue et al. 2002). Reduction of flow in fractures or high-permeability zones after placement of polymer gels has been reported (Seright 1995, 2003a, 2003b; Sydansk 1990; Sydansk and Southwell 2000; Rousseau et al. 2005; Portwood 1999, 2005; Willhite and Pancake 2008).

Polymer gel may enter a fractured formation in its immature (gelant) or preformed mature state, depending on conditions such as wellbore heating and pumping time. Gelant has low viscosity and small particles, which enable it to flow through the rock matrix as well as fractures (Seright et al. 2003), and relatively low pressure gradients are required for extrusion. Subjecting gelant to an elevated temperature over time changes the solution properties and forms a rigid gel. Mature gel is inhibited from passing through pore throats because of its structure, thus the chemical treatment is contained to open fractures during injection (Seright 2001).

Polymer-gel resistance to washout from fractures was previously studied after placement of both immature (Ganguly et al. 2002; Wilton and Asghari 2007) and mature gel (Seright 2003a, 2003b). Ganguly et al. (2002) placed gelant in fractured cores and slabs, with and without gelant intrusion to the matrix. The gel was crosslinked in situ, and the rupture pressure measured during subsequent brine injection. Ganguly et al. (2002) argue that gelant penetrates both the fracture and adjacent rock matrix during injection, thus forming a zone of homogeneous concentrated gel. This creates a gripping effect between gel in the fracture and matrix that may increase the overall pressure resistance of the gel. They did not achieve gelation (crosslinking to form rigid gel) when gelant was placed in the fracture without penetrating the adjacent matrix, presumably because of diffusion of chromium through the porous rock. Gelant may experience compositional changes when contacting reservoir fluids or rock that may interfere with gelation (Zou et al. 2000; Ganguly et al. 2002). In contrast, mature gel shows little sensitivity toward physiochemical conditions in reservoirs (Zhang and Bai 2011). Wilton and Asghari (2007) achieved in-situ gelation, without placing gelant in the matrix adjacent to the fracture, by preflushing the core with chromium solution or by placing gelant with an increased amount of chromium in the fracture (chromium overload).

Seright (1995, 1999, 2001, 2003a, 2003b), Seright et al. (1998), and Seright et al. (2003) showed that preformed gel dehydrates during propagation through a fracture. During the leakoff process, solvent leaves the gel and proceeds through the matrix. The high-concentration gel left in the fracture is more rigid and has a higher pressure resistance than gel of injected composition. Fresh gel flows through the concentrated gel (which has a much lower mobility than the injected gel) in designated flow channels called *wormholes*. The fresh gel contained in the wormholes may be readily mobilized during subsequent waterfloods. Seright (2003a, 2003b) injected mature gel into 1-mm fractures and recorded rupture pressures during subsequent injection of brine or oil.

In the previous work, fracture apertures, experimental setups, and measured gel resistance to washout varied, hence the results were not directly comparable. However, the papers rendered important discussions regarding gel-blocking ability as a function of

Copyright © 2015 Society of Petroleum Engineers

This paper (SPE 169064) was accepted for presentation at the SPE Improved Oil Recovery Symposium, Tulsa, 12–16 April 2014, and revised for publication. Original manuscript received for review 28 April 2014. Revised manuscript received for review 25 January 2015. Paper peer approved 29 January 2015.

gel maturity during placement. This study aimed to reproduce and improve results through core studies. We used four outcrop rock materials, constituting a total of 37 core plugs, to study rupture pressures after placement of gelant crosslinked in situ and of mature gel in open fractures. The unified method of core assembly, comparable core dimensions, and comparable experimental setups, as well as repeated experiments, enabled us to compare results directly on placement of immature and mature gel in fractures and to compare their indications on gel-blocking ability during chase floods.

Experiments

Fractured core plugs were used in this study. The core materials used were Bentheim sandstone (Klein and Reuschlé 2003; Schutjens et al. 1995), Berea sandstone (Churcher et al. 1991), Edwards limestone (Ekdale and Bromley 1993; Tipura 2008; Riskedal 2008), and Portland chalk (Hjuler 2007). Portland chalk cores had approximately 46% porosity and permeability values ranging from 1 to 10 md, whereas the sandstone core materials had porosities of 23% and permeabilities of 500 (Berea) to 1,200 md (Bentheim). The Edwards limestone core material was more heterogeneous in terms of porosity and permeability, and the corresponding values were 15 to 25% and 3 to 28 md, respectively. The cores were cut with a band saw, which created smooth, longitudinal fractures through the core plugs. Earlier work during extrusion of Cr(III)-acetate-hydrolyzed polyacrylamide (HPAM) gels revealed no difference in behavior between cracked fractures (with a rough surface) and smooth fractures (Seright 1995, 1999, 2001). A constant 1-mm fracture aperture was created by placing polyoxymethylene (POM) spacers at the top and bottom of the fracture during core assembly. The core plugs were fitted with POM end pieces, and in some cases matrix taps, and were coated in several layers of epoxy. The core plugs were saturated with Ekofisk brine or gelant under vacuum, and the porosity and pore volume were calculated from weight measurements. The general experimental schedule for all core plugs was as follows:

1. Gel placement by use of gel in its immature or mature state
2. Shut-in period
3. Waterflooding

The aqueous gel/gelant used was a 0.5% 5-million-molecular-weight HPAM, crosslinked by 0.0417% Cr(III) acetate, and the solvent was synthetic Ekofisk brine (4 wt% NaCl, 0.5 wt% MgCl₂·6H₂O, and 3.4 wt% CaCl₂·2H₂O). The high concentrations of divalent cations may seem unusual, but this brine is characteristic of that found in the Ekofisk field, which is the ultimate location that we have in mind for field application of our results. Some of the authors are currently investigating the impact of salinity on gel properties. In the experiments performed to date (shorter periods of time), there is no evidence of decrease in gel strength caused by salinity. Mature gel with a base of high-salinity formation brine has not yielded significantly different leakoff rates or rupture pressures compared with gel mixed in 5% NaCl brine (as in previous work by Seright). We have used a 24-hour-long shut-in period in these experiments to ensure crosslinking of the gel. Bulk volumes of gel have crosslinked within this time frame in all experiments. For immature-gel experiments, salinity has not impacted solution viscosity, and the gel-placement process was comparable with gels with lower salinity content.

The gel was aged for 24 hours (five times gel time) at 41 °C, either before or after placement in fractured core plugs. Two polymer-gel-placement methods were investigated (mature-gel injection into fractured core plugs and injection of gelant solution or direct gelant saturation of fractured cores under vacuum), and these are discussed separately. A shut-in period of 24 hours was conducted after gel placement, during which the cores were left at room temperature (following mature-gel injection) or placed in a heating cabinet at 41 °C to induce gelation.

The objective of the gel placement was to reduce the flow in fractures during chase waterfloods. The gel-blockage performance was assessed before and after gel rupture; the rupture pressure was defined as “the highest initial pressure response observed at

low flow rate before brine breakthrough occurs” (Wilton and Asghari 2007). Rupture pressures were measured by injecting water at the core inlet until the gel in the fracture ruptured and gel and/or water was produced out of the fracture outlet. A sharp drop in the differential pressure was observed, usually at the point of gel rupture. After rupture, gel residing in the fracture continued to reduce fracture permeability. The permeability reduction was measured by flooding water continuously through the fracture at different injection rates and measuring the differential pressure across the fracture.

Mature-Gel Experiments. Varying volumes of formed gel were injected into Fractured-Core Plugs 1 through 16 (**Table 1**) by use of injection rates ranging between 6 and 200 mL/h. An overview of the core properties and associated injection rates can be found in Table 1. The core setup used is shown in **Fig. 1a**. During gel injection, the matrix taps and fracture outlet were open to record the rate of solvent leakoff during gel extrusion through the fracture volume (FV). Gel injection was performed at ambient temperature or an elevated temperature of 41 °C. These temperature differences do not affect the gel behavior in terms of leakoff (Seright 2003a, 2003b). The core plugs were shut in for 24 hours at ambient temperature after gel injection.

To measure the blocking ability of the gel, brine was injected at the inlet end of the core plugs. A constant rate of 6 mL/h (equivalent to 0.23 to 0.42 ft/D if all flow was through the matrix, and equivalent to 9.2 to 12.4 ft/D if all flow was through the fracture only) was first used to measure the rupture pressure. The differential pressure was logged and the rupture pressure recorded at the time of gel rupture, where the passage of fluids through the gel-filled fracture resumed. All matrix taps were closed during water injection. In chosen core plugs, water injection continued to establish a steady state, and the pressure gradient was recorded. The water-injection rate was thereafter adjusted stepwise, and pressure gradients recorded for each rate. The maximum injection rate during brine injection was 600 mL/h (equivalent to 23 to 42 ft/D if all flow was through the matrix, and equivalent to 922 to 1,240 ft/D if all flow was through the fracture only) because of pumping-capacity limitations.

Immature-Gel (Gelant) Experiments. Gelant was injected into Fractured Core Plugs A through U (**Table 2**) at ambient temperature, at a constant injection rate of 30 mL/h, and with a variety of injection schemes to control the gelant saturation in the core.

Saturation Scheme 1. The core setup is shown in **Fig. 1a**. Initially, the matrix taps at the outlet end were open and the fracture outlet was closed. This allowed gelant to flood the matrix in part during injection, although a gradient in gelant saturation will exist through the core. Gelant was injected until breakthrough was observed from both matrix taps. The matrix taps were then closed and the outlet was opened, and gelant was injected through the fracture until breakthrough at the outlet.

Saturation Scheme 2. The core setup was improved by placing matrix taps in the middle of each matrix half, as shown in **Fig. 1b**. Gelant was injected through the top matrix tap until breakthrough at both ends of the fracture. The fracture inlet and outlet were closed, and injection continued until gelant breakthrough in the lower matrix tap.

Saturation Scheme 3. To ensure maximum penetration of gelant to the matrix, matrix taps were placed at the inlet, middle, and outlet of each core half. Gelant was injected as shown in **Fig. 1c**: (I) through the inlet matrix tap of one core half to the outlet matrix half of the other core half, (II) through the other inlet matrix tap to the opposite outlet matrix tap, and (III) following the core setup in Saturation Scheme 2.

Saturation Scheme 4. The core plugs were saturated directly with gelant under vacuum. Core properties and associated saturation schemes are given in Table 2. During gelant injection in Saturation Schemes 1 through 3, gelant breakthrough from the matrix taps was confirmed by measuring the viscosity of the effluent. In

Core	Material	Length (ft)	Diameter (ft)	Porosity (%)	Pore Volume (mL)	Gel Throughput (FV)	Gel- Injection Rate (mL/h)	Rupture Pressure (psi/ft)
1	Bentheim SS	0.34	0.12	22.77	26.52	20.77	6	73.36
2	Portland chalk	0.33	0.13	45.19	52.75	98.25	6	13.48
3	Bentheim SS	0.33	0.13	27.55	31.62	105.47	6	20.05
4	Composite core	0.19	0.17	44.55	52.33	6.14	60	3.25
5	Bentheim SS	0.46	0.17	25.54	72.47	37.11	60	7.76
6	Bentheim SS	0.46	0.17	25.61	72.66	41.46	60	8.17
7	Bentheim SS	0.49	0.17	22.19	68.49	85.15	60	6.09
8	Bentheim SS	0.49	0.17	26.06	80.59	117.90	60	13.10
9	Portland chalk	0.23	0.17	44.91	65.59	197.12	60	36.35
10	Bentheim SS	0.31	0.12	22.72	24.46	4.00	180	6.61
11	Bentheim SS	0.46	0.17	25.61	72.66	41.55	180	6.68
12	Bentheim SS	0.48	0.17	24.03	72.15	81.38	180	14.56
13	Portland chalk	0.26	0.16	48.00	69.90	3.20	200	8.68
14	Bentheim SS	0.48	0.17	24.75	75.11	80.11	200	6.75
15	Composite core	0.46	0.12	34.03	54.10	178.51	200	15.12
16	Composite core	0.32	0.12	36.72	40.65	248.28	200	14.73

Table 1—Cores for mature-gel injection; composite cores are one-half Bentheim sandstone (Bentheim SS) and one-half Portland chalk.

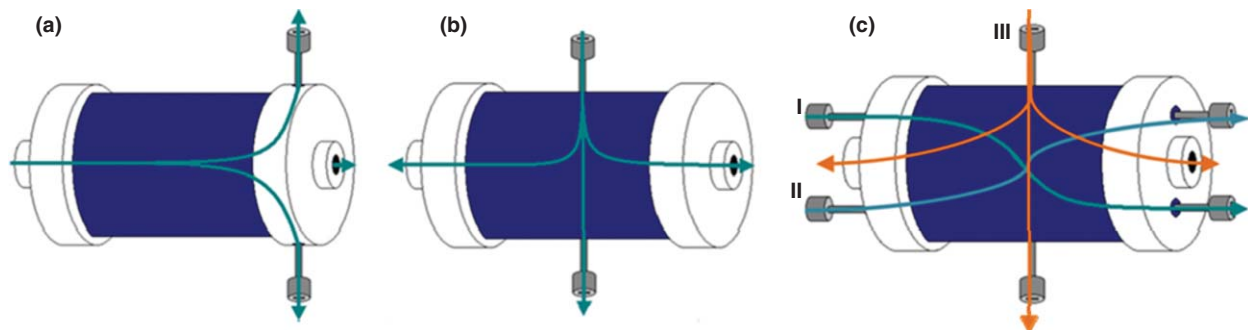


Fig. 1—(a) Core setup used for mature- and immature-gel injection, (b) setup for improved gelant injection, and (c) further improvement of setup for gelant injection to ensure maximum penetration of the matrix.

most cores, 1.5 to 2.5 pore volumes (PV) of gelant solution was injected.

In choosing the injection rate of 30 mL/h for gelant placement, we wanted to use a flow rate that was low enough not to damage the gel during propagation through the matrix, and at the same time, not so low that gelation occurred in part during gelant injection. Hence, 30 mL/h was used. It is possible that a higher flow rate would provide improved gelant saturation, and as such, close the gap between the saturation schemes. However, gelant saturation in the matrix was improved by altering the core setups instead of altering the rate.

The partially or fully gelant-saturated core plugs were placed in an oven at 40 to 48 °C for 24 hours (five times the gelation time) to allow gelation. Effluent samples taken from the matrix outlets were also placed in the oven to confirm crosslinking of the injected gelant solution. After shut-in, the cores were then cooled to ambient temperature, and water was injected at 6 mL/h until the gel ruptured and the rupture pressure was recorded. All matrix taps were closed during water injection. In some cases, water injection continued and the pressure differential across the fracture was recorded for several increasing and/or decreasing rates at steady states.

Core Plugs E through Q were tested a second time immediately following the first test. Gelant was placed in the fracture volume only (without core matrix taps open to promote gelant leakoff to the matrix), and gelation occurred in situ during the 24-hour shut-in period. This was done to ensure limited interactions

with the rock matrix during second-time gelant placement and to investigate the rupture pressure achieved without gelant leakoff. The same waterflooding procedure was followed.

Results and Discussion

Mature-Gel Experiments. The measured leakoff rates during gel injection are shown in Fig. 2a, and the pressure gradients are shown in Fig. 2b. The leakoff rates corresponded with the filter-cake model (Seright 2003a, 2003b) for injection rates of 180 to 200 mL/h. For gel-injection rates ≤ 60 mL/h, leakoff rates fell below the filter-cake model, and, by use of the lowest injection rate of 6 mL/h, the leakoff rate was linear until gel breakthrough at the fracture outlet, at which point it decreased abruptly and was thereafter measured to be a lower parallel to the filter-cake model. The measured leakoff rates were independent of core material. In Cores 1, 4, 10, and 13, gel was injected until breakthrough at the outlet end of the fracture only, and the leakoff rates were therefore not measured. The achieved differential-pressure gradients during mature-gel injection were between 10 and 60 psi/ft. The plateau pressures achieved varied within each injection rate. A variation in plateau pressure was also observed previously by Seright (2003a, 2003b), who concluded that the achieved pressure plateaus were controlled largely by the fracture width, rather than the applied injection rate. The time it took for the pressure to build up to plateau varied on the basis of the injection rate, and is illustrated by the red square in Fig. 2b. The time required to reach the

Core	Material	Length (ft)	Diameter (ft)	Porosity (%)	Pore Volume (mL)	Saturation Scheme	Rupture Pressure P_R (psi/ft)	Second Rupture Pressure P_R (psi/ft)
A	Bentheim SS	0.46	0.17	25.8	73.23	1	0.63	NM
B	Bentheim SS	0.46	0.17	22.9	64.93	1	0.21	NM
C	Bentheim SS	0.46	0.17	24.1	68.37	1	NA	NM
D	Bentheim SS	0.46	0.17	18.4	52.24	1	NA	NM
E**	Bentheim SS	0.49	0.17	22.7	70.53	2	0.62	0.56*
F	Bentheim SS	0.49	0.17	23.5	73.40	2	0.36*	0.50*
G	Bentheim SS	0.49	0.17	22.1	67.71	2	0.07*	3.18
H	Edwards LS	0.24	0.17	26.5	39.35	3	3.63	3.71
I	Edwards LS	0.24	0.17	28.3	41.70	3	15.03	3.71
J	Edwards LS	0.23	0.17	24.9	37.21	3	12.38	8.84
K	Edwards LS	0.23	0.17	26.5	38.93	3	6.19	7.96
L	Bentheim SS	0.50	0.17	21.7	68.89	4	0.18*	1.02
M	Bentheim SS	0.49	0.17	23.5	73.31	4	2.61	1.15
N	Bentheim SS	0.49	0.17	24.0	74.91	4	0.14*	0.44
O	Berea SS	0.24	0.16	22.1	31.61	4	12.38	11.94
P	Berea SS	0.23	0.16	32.6	45.32	4	16.80	NM
Q	Berea SS	0.24	0.16	26.4	37.24	4	26.97	3.80
R	Edwards LS	0.23	0.16	29.0	39.56	4	53.05	NM
S	Edwards LS	0.24	0.16	29.7	40.40	4	25.64	NM
T	Edwards LS	0.23	0.16	29.1	39.33	4	14.59	NM
U	Edwards LS	0.24	0.16	28.0	38.51	4	17.68	7.52

NA = not achieved.

NM = not measured.

*The rupture pressure was not clearly defined. The value given is the highest pressure obtained during water injection with the lowest rate.

**Core E was flooded with a 0.0417% Cr(III)-acetate solution before gelant injection.

Table 2—Cores for gelant placement and in-situ crosslinking.

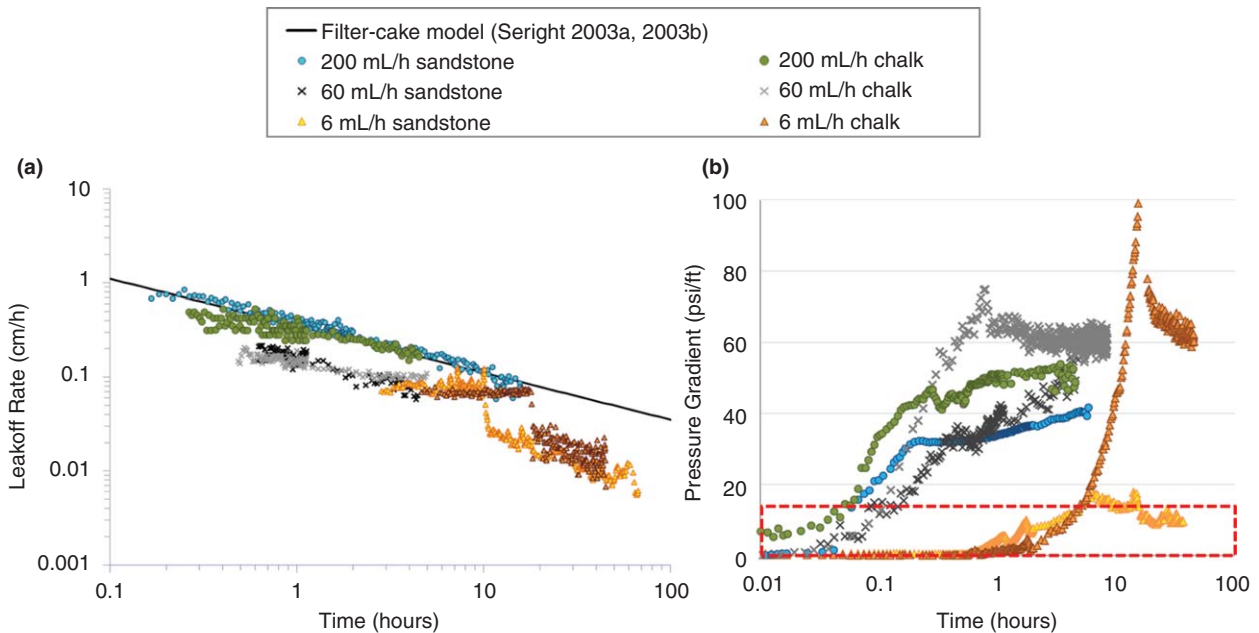


Fig. 2—(a) Measured leakoff rates during mature-gel injection in fractured core plugs. (b) Differential-pressure gradients during gel injection. Triangles illustrate cores in which a gel-injection rate of 6 mL/h was used, crosses illustrate a 60-mL/h injection rate, and circles denote cores in which gel was injected at 200 mL/h. The red square illustrates rate dependency; the plateau differential pressure is not influenced by gel-injection rate, but it takes a longer time period to build up to the plateau when the injection rate is lower.

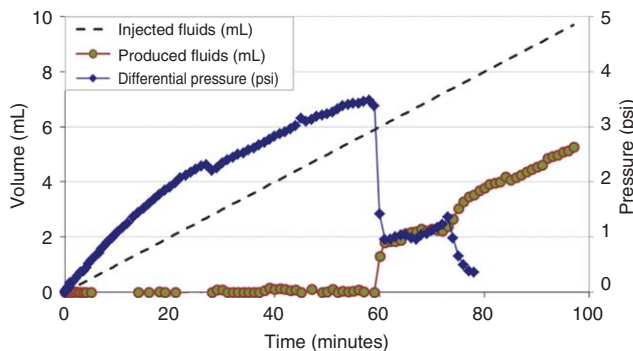


Fig. 3—Rupture pressure for Core 2. The distinct pressure drop at $t \approx 60$ minutes corresponded with rupture of the gel and production of fluids from the fracture outlet.

plateau pressure was approximately 0.2 hours for a 200-mL/h injection rate, 1 hour for a 60-mL/h injection rate, and 14 hours for a low gel-injection rate of 6 mL/h.

After gel injection, the cores were shut in for 24 hours. Brine was thereafter injected at a lower, constant rate of 6 mL/h and the rupture pressure was recorded. Fig. 3 shows the rupture-pressure measurement for Core 2. The defined pressure drop corresponded with rupture of the gel and production of fluids from the fracture outlet.

Measured rupture pressures, following mature-gel injection and shut-in, varied from 3.3 to 73.4 psi/ft, and were observed to vary on the basis of the gel-placement rate and gel throughput. Increasing rupture pressures with gel throughput were observed for specific gel-injection rates of 60, 180, and 200 mL/h. The injection rates yielded similar rupture pressures up to approximately 70 FV injected, after which, a lower gel-injection rate generally yielded a higher rupture pressure at the same number of gel FVs injected. The trend was clearer after injection of several FVs of gel and not evident when gel was injected until breakthrough only. It took 3.2, 4.0, 6.1, and 20.8 FV of gel to reach the fracture outlet when the injection rates were 200, 180, 60, and 6 mL/h, respectively. The recorded rupture pressures after shut-in were 8.68, 6.01, 3.25, and 73.36 psi/ft, respectively. The high rupture pressure measured after filling the fracture with gel at 6 mL/h was not reproduced by increasing the gel throughput at this injection rate.

Fig. 4 shows the rupture pressures achieved and the linear trends between measured rupture pressures and injected-gel volumes when gel-placement rates were held constant at 60 mL/h (Fig. 4a) and at 180 and 200 mL/h (Fig. 4b), respectively, and gel throughput varied.

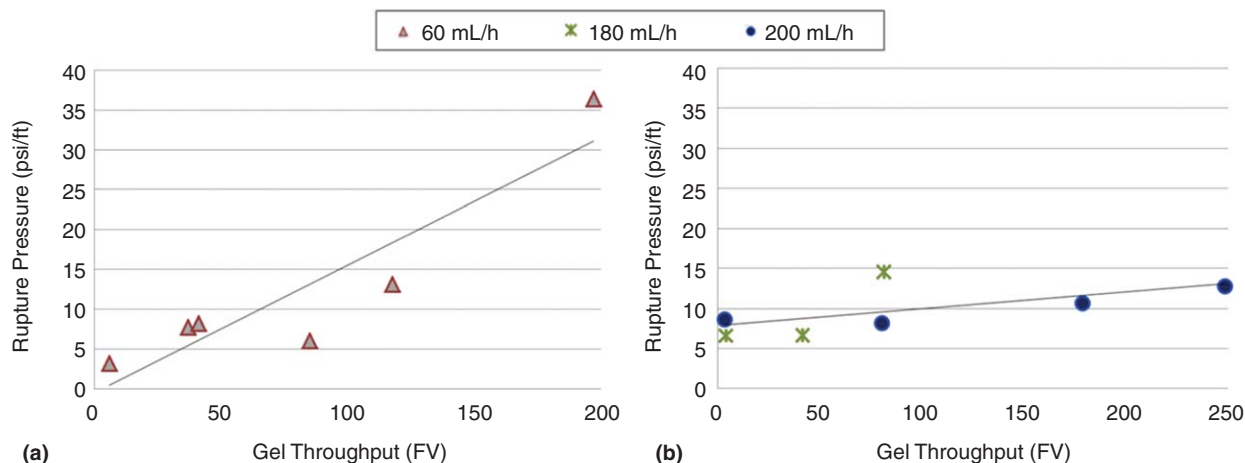


Fig. 4—(a) Rupture pressure as a function of injected FVs of gel at a 60-mL/h placement rate. (b) Rupture pressure as a function of FVs of gel injected at 200 mL/h. Data points for injection at 180 mL/h are also included.

Immature-Gel (Gelant) Experiments. A wide variety of rupture pressures was achieved when gelant was injected into fractured cores and crosslinked in situ. Fig. 5 shows the achieved rupture pressures and illustrates the improvement in results as gelant saturation in the cores increased. In some cores, pressure buildup was seen during water injection, although rupture pressures were not defined clearly (i.e., no abrupt drop in pressure coincided with production of gel or water from the fracture outlet). In such cases, the highest pressures obtained during low-rate water injection (before water breakthrough at the fracture outlet) were recorded and marked with an asterisk (*) in Table 2.

Four cores were saturated by use of Saturation Scheme 1 (SS 1; see Fig. 1a). Low rupture pressures below 1 psi/ft were recorded during subsequent water injection. For the three cores saturated by use of Saturation Scheme 2 (SS 2; see Fig. 1b), rupture pressures were also below 1 psi/ft after the first gel placement. The highest rupture pressure of 0.62 psi/ft was measured for Core E, which was preflushed with Cr(III) solution. Four cores were saturated by use of Saturation Scheme 3 (SS 3; see Fig. 1c), and 10 cores were saturated by use of Saturation Scheme 4 (SS 4; core vacuum saturated with gelant). The rupture pressures generally increased with increased gelant saturation of the matrix (increasing the saturation-scheme number); however, variation within each saturation scheme was also observed. The highest rupture pressure achieved was 53.05 psi/ft, measured after direct saturation of cores with gelant under vacuum (SS 4). The results of these experiments illustrate that the gelant saturation in the matrix is important and influences the gel-blocking capacity during chase floods significantly. The experiments may have been less illustrative if the “gaps” between gelant-saturation values were lower (e.g., by use of higher gelant-injection rates).

The core permeability should not influence the rupture pressure of the gel in the fractures in these experiments for the following reasons:

1. During immature-gel injection, a fraction of the core matrix was filled forcibly with immature gel during gel placement. In the majority of cores, this gel was assumed to crosslink during shut-in and rendered the fracture and adjacent matrix impermeable or caused significantly lower permeability.
2. During subsequent water injection, matrix taps were closed.

We can therefore assume that all injected water only moved through the fracture in these experiments. The permeability of the gel in the fracture was found previously to vary on the basis of the gel concentration, and therefore, does not vary between the experiments in which immature gel was placed in the core, and the gel concentration is believed to be uniform (Seright 2003a, 2003b).

Gel Failure After Gelant Placement. Low rupture pressures were most frequently observed in Bentheim sandstone core plugs, when the matrix was only partly saturated with gelant (SS 1 and

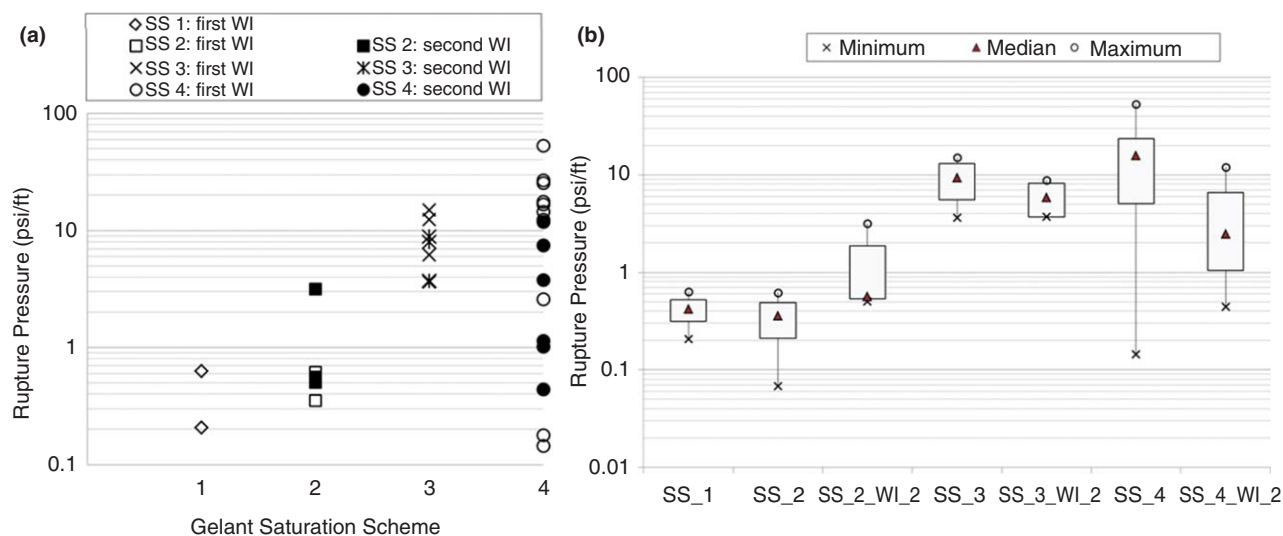


Fig. 5—(a) Rupture pressures achieved during water injection after placement and in-situ crosslinking of gelant. WI denotes water injection. (b) Results shown as a box plot, with the boxes representing the values within the 25 to 75% range.

SS 2, see Figs. 1a and 1b). Where pressure buildup was not attained, we observed that polymer solution rather than gel was displaced from the fracture. The large variation in rupture pressures may be caused by fluid/rock interactions, resulting in chromium precipitation (Zou et al. 2000). Chromium precipitation from the gelant to the rock causes the chromium concentration in the resulting gelant solution to be too low to form gel (Ganguly et al. 2002). To determine if contact with the core materials led to compositional changes in the gelant and failed gelation, Bentheim sandstone, Edwards limestone, and Portland chalk core material were crushed and mixed with gelant in individual beakers. The samples were incubated at 41 °C to start gelation. The gelant solution crosslinked and formed gel when mixed with fragments of Edwards limestone and Portland chalk, but the Bentheim sandstone material and fluids reacted and gel was not formed. Efforts were made to determine whether lack of gelation in the Bentheim cores was caused by chromium precipitation, but results were not conclusive. pH levels in a gelant solution mixed with crushed Bentheim sandstone core material were measured during gelation, and Core E was flooded with a chromium-acetate solution [0.0417 wt% Cr(III)-acetate] before gelant injection to limit possible diffusion. The pH levels of the gelant solution were found to be uniform throughout the gelation time when mixed with Bentheim sandstone, although gel did not form. Zou et al. (2000) observed that chromium could precipitate from chromium-acetate solutions at constant pH values, thus chromium precipitation may still be a valid explanation. The chromium preflush of Core E before gelant injection did not increase the rupture pressure significantly, and it was recorded at 0.62 psi/ft. Wilton and Asghari (2007) measured rupture pressures between 0.3 and 13.7 psi/ft when fractured slabs were preflushed with chromium solution and gelant was placed in the fracture volume only, without leakoff to the matrix. Other fluid/rock interactions may also have occurred that interfered with in-situ gelation. Bentheim sandstone cores exhibited low rupture pressures when using all saturation schemes, including SS 4, at which uniform chromium concentrations existed throughout the cores after direct saturation of the cores by gelant.

In 13 cores (Cores E through Q), a second placement of gelant in the fractures was performed immediately after rupture-pressure measurements, without matrix taps open to promote leakoff of gelant into the matrix pore volume. The second gelant placement exhibited limited chromium precipitation because the core matrix adjacent to the fracture had already been contacted by chromium. During second-time waterflooding after crosslinking, clear rupture pressures were achieved, and mature gel was produced out of the fracture outlet. Rupture pressures achieved after the second gelant placement ranged between 0.5 and 11.9 psi/ft and were compara-

ble with the measured rupture pressures of Wilton and Asghari (2007), although their fracture system exhibited an initial permeability seven times lower than ours [11,000 darcies compared with 84,000 darcies, calculated by the cubic law (Witherspoon et al. 1980)]. The second rupture pressures were in most cases lower than the first measured P_R . This may be a result of minor gripping between the fracture and adjacent matrix because gel only formed in the fracture and no bonds with gel in the matrix were formed.

Comparison of Results: Gel and Gelant

Fig. 6 summarizes the rupture pressures achieved after immature- and mature-gel placement in 1-mm fractures, compared with the experimental results from gelant placement of Ganguly et al. (2002) and gel placement of Seright (2003a, 2003b). All experimental results from the use of Bentheim sandstone have been omitted from the figure because of uncertainties regarding core-material/fluid-system interactions, causing gelation failure in some cores. The achieved rupture pressures from the use of preformed gel and gel crosslinked in-situ were in the same order of magnitude in this study; although, the use of gelant held more elements of uncertainty than the use of preformed gel. Gelation failure occurred in some cores, and a high gelant saturation in the core material was important to achieve higher rupture pressures. By maximizing gelant saturation in the matrix (by use of SS 4), rupture pressures of 12 to 53 psi/ft were measured. The measured rupture pressures of Ganguly et al. (2002), when using a fracture aperture of 1 mm, were all less than 10 psi/ft. Placing preformed gel in fractures produced clear rupture pressures during chase floods, ranging from 9.1 to 20.3 psi/ft (Seright 2003a, 2003b), and 3.3 to 73.4 psi/ft (this study). Some variability in rupture pressure exists for a given line of data, although the box plots in Fig. 6b illustrate that the majority of rupture pressures are in the same range when preformed gel was used. For gelant, the variability may be attributed to the amount of gelant saturation in the matrix, possible precipitation of chromium, and core material/fluid interactions (although Bentheim cores are omitted in the figure). For gel, rupture-pressure variability may be caused by the variance in injection rates and volumes. Variability in mature-gel experiments is also observed in plateau pressures during gel placements.

Continued Waterflooding After Gel Rupture. In Core 3 ($P_R=20.1$ psi/ft) and Core P ($P_R=16.8$ psi/ft), water injection was continued after the rupture pressure was reached, and the differential pressure was recorded at steady states for several injection rates. The injection rate was stepwise increased, and

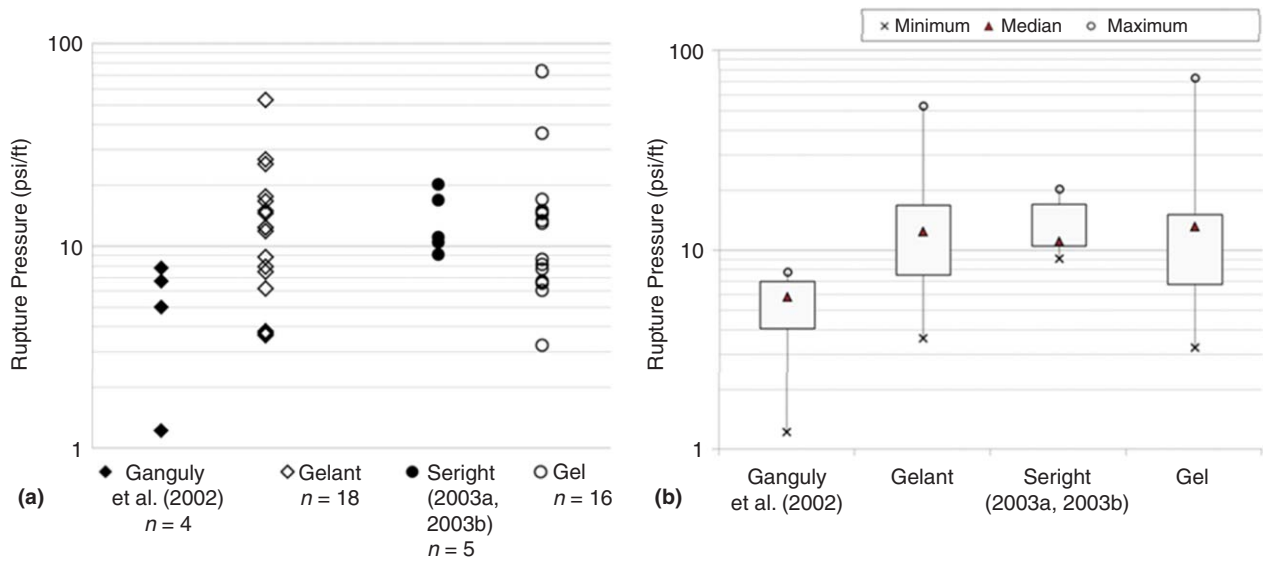


Fig. 6—(a) Rupture pressures measured after placement of mature and immature gel (gelant) compared with the measured rupture pressures of Seright (2003a, 2003b) and Ganguly et al. (2002) in 1-mm fractures. **(b)** Results shown as a box plot, with the boxes representing the majority of measured values.

thereafter, decreased through eight flushes. A flush is here defined as one full sequence of rates, decreasing (starting at the maximum rate) or increasing (starting at the minimum rate). Fig. 7a shows the rate sequences and corresponding measured differential pressure for Core 3 (mature gel), and Fig. 7b shows the injection rates and measured differential pressure across Core P (gelant cross-linked in situ). The differential pressures are normalized to the respective rupture pressure of each core for improved comparison. Fig. 7 shows clearly that the pressure response during waterflooding was higher in Core 3 (mature-gel placement) compared with Core P (immature-gel placement and in-situ crosslinking). This may be explained by gel behavior during placement at the different maturity regimes—mature gel dehydrates during propagation through a fracture, which increases its pressure resistance, and fresh gel flows through the concentrated gel in wormholes. During chase waterflooding, fresh gel is displaced from the wormholes at the rupture pressure, and water follows these narrow flow paths through the fracture. As long as the injected water is contained in wormholes, fracture permeability remains significantly decreased. In Core P, wormholes do not form during immature-gel placement. Consequently, gel erosion during waterflooding occurs in a different manner, and may open larger sections of the fracture to flow.

The maximum pressure gradients measured during water injection at specific rates (6, 60, 300, and 600 mL/h) are represented in Fig. 8 as functions of the effective brine velocity

through the fracture. The pressure gradients in both cores decreased for the first two rates in the first flush (increasing rate), and the decrease was most prominent in Core P. The pressure gradient decreased further during the second and third water flushes. After the third flush, pressure gradients for Core 3 remained stable for injection rates greater than 6 mL/h. Stabilization of the system at 6 mL/h took longer, and the recorded pressure gradient may vary according to how long the system was maintained at the lower rate before proceeding with the next flush. The decrease in pressure gradients was expected and was attributed to erosion of gel in the wormholes during water injection. Stable pressure gradients for the higher specific rates suggest that erosion of gel was minor and even-higher rates would be required to further erode the gel around the wormholes. For Core P, pressure gradients continued to decrease with water throughput, although the pressure gradient was fairly stable for the highest specific rate after the second flush.

After water injection, the cores were taken apart, and the fracture surfaces of Core 3 revealed several wormholes through concentrated gel. Core P fracture surfaces were coated with a thin layer of uniform gel. It is believed that the fracture was filled initially with low-concentration gel, and gradually opened to flow when the gel dehydrated (Krishnan et al. 2000) or was flushed out by water.

Fig. 9 shows the pressure gradients for the specific injection rates as functions of water throughput during the fifth water flush

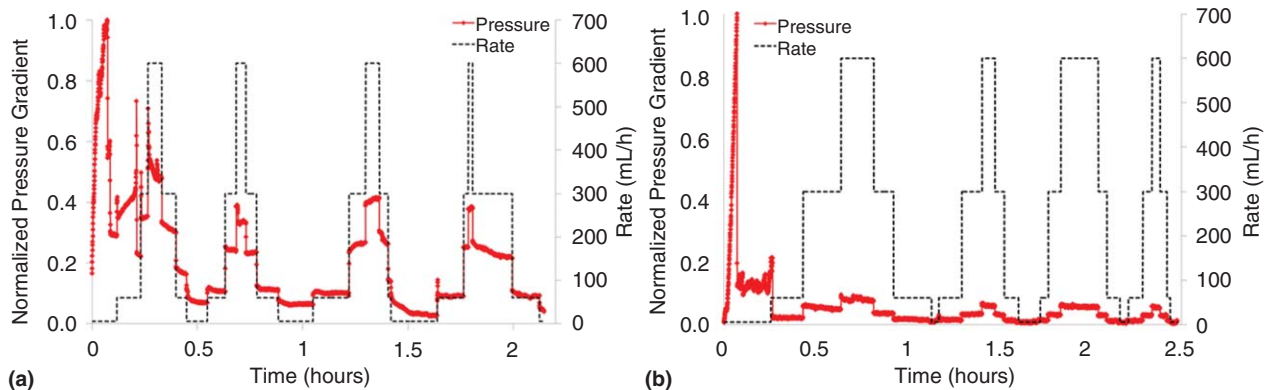


Fig. 7—(a) Rate and differential pressure for Core 3 during water injection after gel injection and shut-in and **(b)** rate and differential pressure of Core P after gelant injection and in-situ crosslinking. The differential pressures are normalized to the respective rupture pressures in each core.

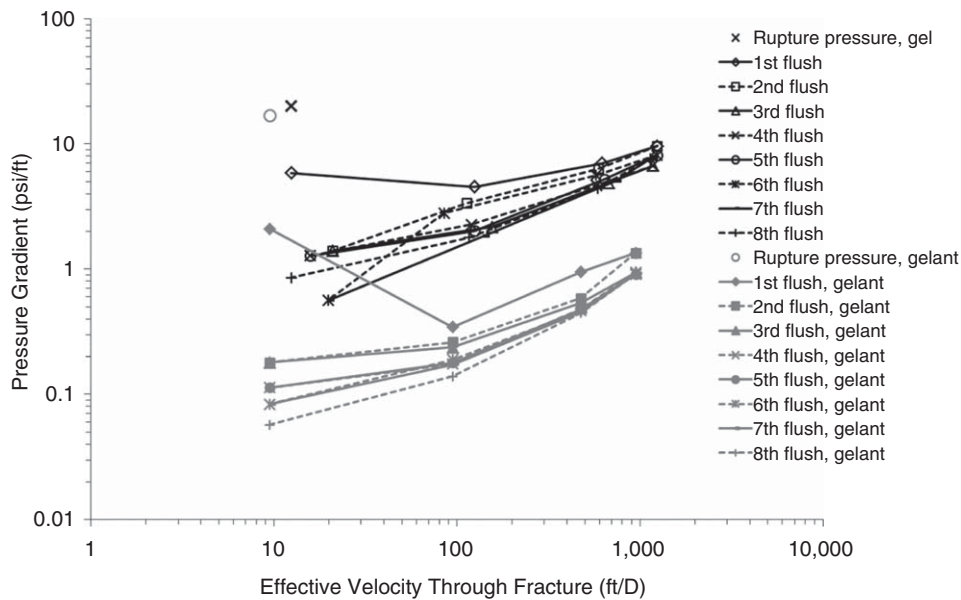


Fig. 8—The pressure gradient plotted against the effective velocity through the fracture for both gel and gelant. Flushes with decreasing rate steps are shown with dotted lines.

of Core 3 and Core P, after the pressure gradients had stabilized in both cores. The achieved pressure gradients were higher in Core 3 (mature gel) compared with Core P (gelant) for all rates. A higher pressure gradient was reached in Core 3 for the low injection rate of 6 mL/h than for an injection rate a hundred times greater (600 mL/h in Core P). The substantially greater pressure resistance of mature gel after rupture, and significant throughput of water, may be explained by the elasticity of the gel, allowing its wormholes to collapse and reopen during waterflooding at the given rates. The effective channel width open to flow (i.e., the wormhole size) in Core 3 during water injection was calculated from (Seright 2003a, 2003b):

$$W_w = \frac{2G'}{\left(\frac{dP}{dL}\right)}, \dots \dots \dots (1)$$

where W_w is the channel width open to flow, G' is the elastic modulus of the gel, and (dP/dL) is the experimentally measured pressure gradient. The calculated W_w is shown in Fig. 10a. Fig. 10b

shows calculated wormhole size from pressure data at the specific rate of 60 mL/h and illustrates the general behavior. Wormhole size increased initially, and thereafter stabilized at a close-to-constant value for several flushes. Continued erosion of wormholes with water throughput was not observed for mature gel after the first few flushes, thus an increase in flow channel width was reversible at the given rates. The gradual opening of a fracture during waterflooding after placement and rupture of immature gel was largely irreversible.

The residual resistance factor to water, F_{rrw} , gives the relationship between water mobility in the fracture before and after gel placement. F_{rrw} values were calculated for Core 3 and Core P waterfloods and are given in Fig. 11a as a function of time and in Fig. 11b as a function of injection rate. Permeability of the fractures before gel treatment was calculated from the cubic law (Witherspoon et al. 1980), and permeability of the system after gel placement was calculated by use of Darcy's law and the measured pressure drop across the fracture. The residual resistance factors for the cores are initially comparable and both decrease some with water throughput, but F_{rrw} for Core P decreases faster than

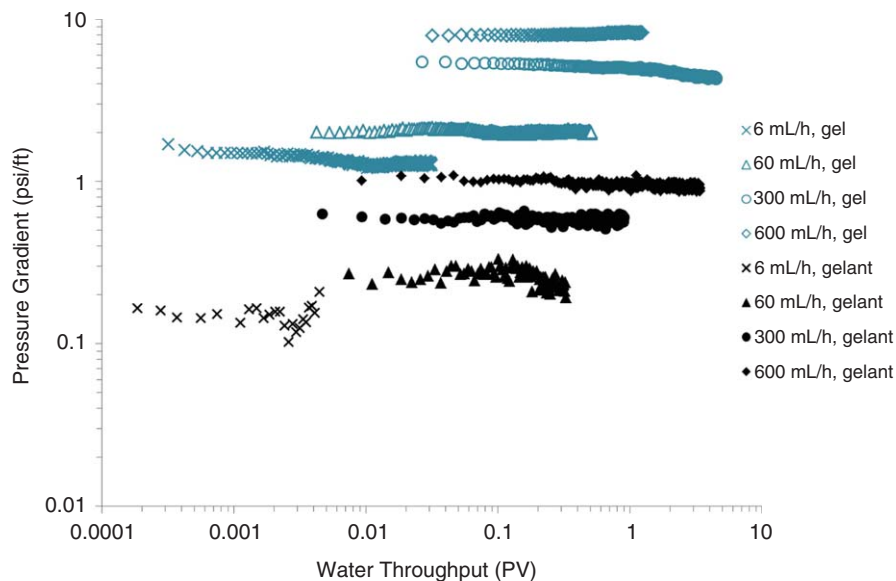


Fig. 9—Pressure gradients for specific injection rates as a function of water throughput for the fifth water flush of Core 3 and Core P.

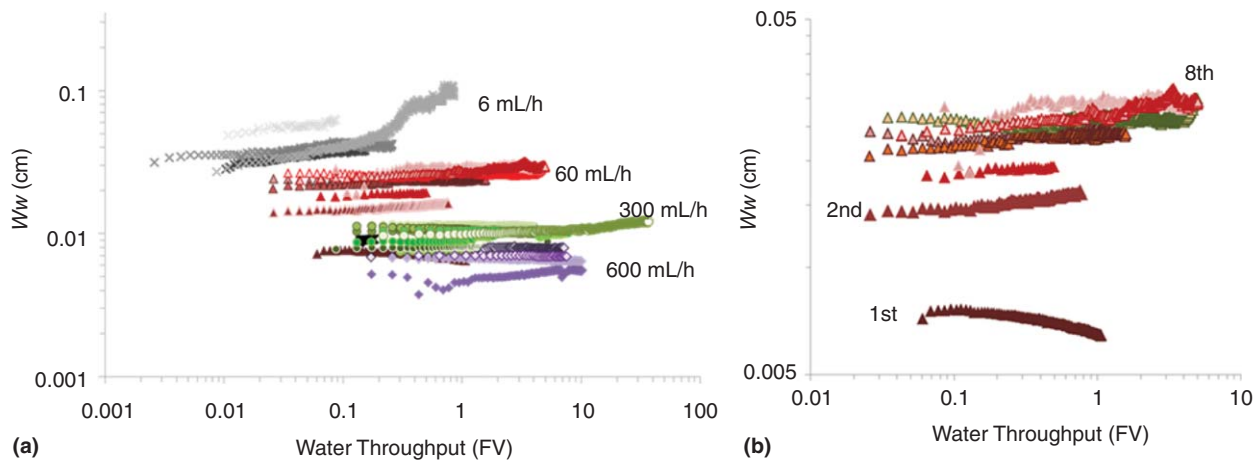


Fig. 10—(a) The effective channel width open to flow during water injection. (b) Effective channel width for specific rate of 60 mL/h.

for Core 3. After the eighth water flush, the permeability reduction in Core 3 (128 FV of water injected) averaged a factor of 5,000 and Core P (170 FV of water injected) averaged a factor of 600. Large-scale variations in system permeability were seen with variations in injection rate. This is expected behavior owing to the elastic nature of the gel (Wilton and Asghari 2007).

Significance to Field Applications. The experiments performed in this study showed that the rupture pressures achieved after gel treatment either with gelant crosslinked in situ or mature, fully formed gel may be in the same order of magnitude. However, injection of gelant holds more elements of uncertainty than injection of preformed gel. Interactions between the fluids and rock material caused gelation failure in some cores, especially where gelant saturation in the matrix was limited. Inability to form a mature gel in cores after placement of immature gel has also been observed previously: Ganguly et al. (2002) proposed that gelation could not occur in fractures if leakoff of gelant to the fracture-adjacent matrix was not attained; however, Wilton and Asghari (2007) showed that leakoff of gelant to the matrix was not necessary, and gel could form if the near-fracture region was preflushed with chromium or when gelant was placed in the fracture with chromium overload. Second-time gelant placement in this study supports the latter findings because gel formed in the fracture without being placed simultaneously in the matrix, presumably because the fracture-adjacent matrix was treated with gelant solution during previous tests.

When, or if, crosslinking after immature-gel (gelant) placement in a fractured system depends on a matrix preflush or intrusion of gelant to the fracture-adjacent matrix during placement, matrix properties will partly control the success of the gel treatment. Res-

ervoirs with highly permeable fractures between connected wells, oil-wet preferences in which the matrix entry pressure is high compared with the differential pressure reached during gelant injection, or where pore throats are too narrow to allow gelant penetration may be particularly challenging and call for use of preformed gel. Placement of preformed gel in open fractures yielded consistent results, and chemical interactions between fluids and rock material were not observed. In most field applications, gelant is mixed at a surface facility and immediately injected through the wellbore. Treatment size and injection time vary, but in most cases, will surpass the inherent short gelation time of the Cr(III)-HPAM gel system of approximately 5 hours at 41 °C. The most successful gel treatments of naturally fractured reservoirs required injection of large volumes of gel, and gel-injection times far exceeding the gelation time (Sydansk and Moore 1992; Borling 1994; Hild and Wackowski 1999). Thus, mature gel extrudes through fractures during most of the placement process.

The level of permeability reduction (i.e., residual resistance factor) during stabilized brine flow after the initial gel rupture is also important in a field application. The local flow capacity of a fracture can be thousands or even millions of times greater than the flow capacity of the surrounding matrix. Especially for moderate-to-wide fractures, large reductions in the flow capacity of the fracture are very desirable. For example, a gel that provides a residual resistance factor (in the fracture) of 5,000 reduces the fracture flow capacity and the extent of channeling through the fracture by 10 times more than a gel that provides a residual resistance factor of only 500.

Future Work. Mature- and immature-gel placement (and crosslinking) in the presence of oil-saturated rock at different

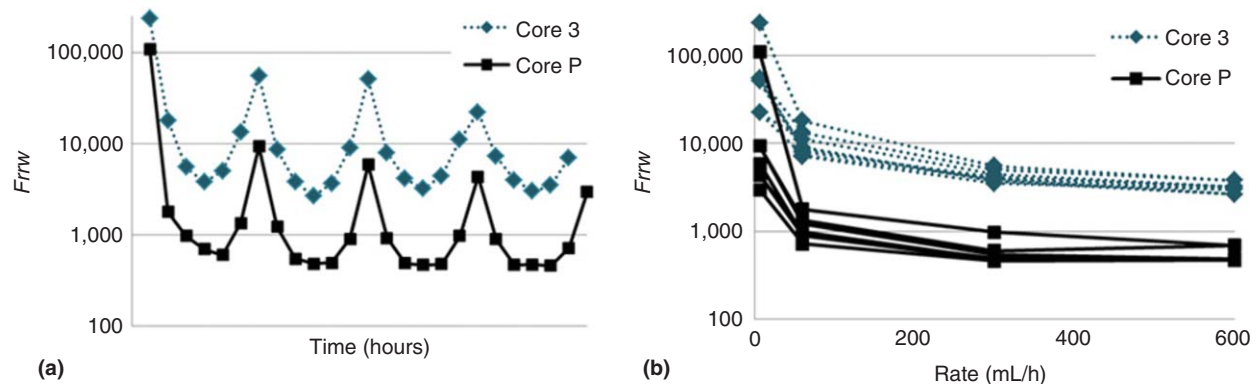


Fig. 11—(a) Residual resistance factor to water for Core 3 and Core P at different specific rates. (b) Residual resistance factor to water as a function of injection rate.

wettabilities should be investigated to improve the understanding of gel behavior in conjunction with real reservoir rock.

Conclusions

- Placement of mature gel in open fractures yielded consistent rupture pressures during subsequent water injections, following linear trends for given gel-placement rates and throughput volumes.
- Rupture pressures achieved after placement and in-situ cross-linking of gelant were comparable with mature-gel rupture pressures, but were less predictable. When maximizing gelant saturation in the matrix, rupture pressures were measured to be 12 to 53 psi/ft, excluding Bentheim sandstone cores, where interactions between core material and gelant were observed.
- The maximum achieved rupture pressure when gelant was placed without matrix taps to promote leakoff was 11.9 psi/ft.
- Interactions between rock material and gelant were observed when Bentheim sandstone cores were used, and gel did not form in some cores. No such interactions were observed in experiments that used formed gel.
- Gel placed in fractures limited permeability to water after rupture when placed as both gel and gelant. Residual resistance factors for cores treated with gel and gelant were comparable initially. After eight water flushes (> 120 FV water injected), substantially greater pressure gradients were observed in cores treated with formed gel than with gelant crosslinked in situ, and the permeability reduction averaged a factor of 5,000 for gel-treated cores and 600 for gelant-treated cores.

Nomenclature

dP/dL = experimentally measured pressure gradient, p/L, m/L^2t^2 , psi/ft

F_{rrw} = residual resistance factor to water, conductivity before gel treatment/conductivity after gel treatment, cm^2/cm^2

G' = elastic modulus of the gel, G' = stress/strain, psi

P_R = rupture pressure, p/L, m/L^2t^2 , psi/ft

W_w = wormhole size, channel width open to flow, d, cm

Acknowledgments

The authors wish to thank Stephen J. Johnson and Karen Peltier of the Tertiary Oil Recovery Program at the University of Kansas, and Kathryn Wavrik at the Petroleum Recovery Research Center of New Mexico Tech for guidance and help during experiments. The authors at the Department of Physics and Technology, University of Bergen, are grateful to the Norwegian Research Council for financial support.

References

Borling, D. C. 1994. Injection Conformance Control Case Histories Using Gels at the Wertz Field CO₂ Tertiary Flood in Wyoming. Presented at the SPE/DOE Improved Oil Recovery Symposium, Tulsa, 17–20 April. SPE-27825-MS. <http://dx.doi.org/10.2118/27825-MS>.

Churcher, P. L., French, P. R., Shaw, J. C. et al. 1991. Rock Properties of Berea Sandstone, Baker Dolomite, and Indiana Limestone. Presented at the SPE International Symposium on Oilfield Chemistry, Anaheim, California, USA, 20–22 February. SPE-21044-MS. <http://dx.doi.org/10.2118/21044-MS>.

Ekdale, A. A. and Bromley, R. G. 1993. Trace Fossils and Ichnofabric in the Kjølbj Gaard Marl, Uppermost Cretaceous, Denmark. *Bull Geol Soc Denmark* **31**: 107–119.

Ganguly, S., Willhite, G. P., Green, D. W. et al. 2002. The Effect of Fluid Leakoff on Gel Placement and Gel Stability in Fractures. *SPE J.* **7** (3): 309–315. SPE-79402-PA. <http://dx.doi.org/10.2118/79402-PA>.

Graue, A., Nesse, K., Baldwin, B. A. et al. 2002. Impact of Fracture Permeability on Oil Recovery in Moderately Water-Wet Fractured Chalk Reservoirs. Presented at the SPE/DOE Improved Oil Recovery Symposium, Tulsa, 13–17 April. SPE-75165-MS. <http://dx.doi.org/10.2118/75165-MS>.

Hild, G. P. and Wackowski, R. K. 1999. Reservoir Polymer Gel Treatments To Improve Miscible CO₂ Flood. *SPE Res Eval & Eng* **2** (2): 196–204. SPE-56008-PA. <http://dx.doi.org/10.2118/56008-PA>.

Hjuler, M. L. 2007. *Diagenesis of Upper Cretaceous Onshore and Offshore Chalk from the North Sea Area*. PhD dissertation, Technical University of Denmark, Copenhagen, Denmark (August 2007).

Klein, E. and Reuschlé, T. 2003. A Model for the Mechanical Behaviour of Bentheim Sandstone in the Brittle Regime. *Pure Appl Geophys* **160** (5): 833–849. <http://dx.doi.org/10.1007/pi00012568>.

Krishnan, P., Asghari, K., Willhite, G. P. et al. 2000. Dehydration and Permeability of Gels Used in In-Situ Permeability Modification Treatments. Presented at the SPE/DOE Improved Oil Recovery Symposium, Tulsa, 3–5 April. SPE-59347-MS. <http://dx.doi.org/10.2118/59347-MS>.

Portwood, J. T. 1999. Lessons Learned from over 300 Producing Well Water Shut-Off Gel Treatments. Presented at the SPE Mid-Continent Operations Symposium, Oklahoma City, Oklahoma, USA, 28–31 March. SPE-52127-MS. <http://dx.doi.org/10.2118/52127-MS>.

Portwood, J. T. 2005. The Kansas Arbuckle Formation: Performance Evaluation and Lessons Learned from More Than 200 Polymer-Gel Water-Shutoff Treatments. Presented at the SPE Production Operations Symposium, Oklahoma City, Oklahoma, USA, 16–19 April. SPE-94096-MS. <http://dx.doi.org/10.2118/94096-MS>.

Riskedal, H. 2008. *Wettability and Rock Characterization of Heterogeneous Limestone Utilizing NMR*. MS thesis, University of Bergen, Bergen, Norway (April 2008).

Rousseau, D., Chauveteau, G., Renard, M. et al. 2005. Rheology and Transport in Porous Media of New Water Shutoff/Conformance Control Microgels. Presented at the SPE International Symposium on Oilfield Chemistry, The Woodlands, Texas, USA, 2–4 February. SPE-93254-MS. <http://dx.doi.org/10.2118/93254-MS>.

Schutjens, P. M. T. M., Hausenblas, M., Dijkshoorn, M. et al. 1995. The Influence of Intergranular Microcracks on the Petrophysical Properties of Sandstone—Experiments to Quantify Effects of Core Damage. Presented at the International Conference for the Society of Core Analysts, San Francisco, SCA-9524.

Seright, R. S. 1995. Gel Placement in Fractured Systems. *SPE Prod & Fac* **10** (4): 241–248. SPE-27740-PA. <http://dx.doi.org/10.2118/27740-PA>.

Seright, R. S. 1999. Polymer Gel Dehydration During Extrusion Through Fractures. *SPE Prod & Fac* **14** (2): 110–116. SPE-56126-PA. <http://dx.doi.org/10.2118/56126-PA>.

Seright, R. S. 2001. Gel Propagation through Fractures. *SPE Prod & Fac* **16** (4): 225–231. SPE-74602-PA. <http://dx.doi.org/10.2118/74602-PA>.

Seright, R. S. 2003a. An Alternative View of Filter-Cake Formation in Fractures Inspired by Cr(III)-Acetate-HPAM Gel Extrusion. *SPE Prod & Fac* **18** (1): 65–72. SPE-81829-PA. <http://dx.doi.org/10.2118/81829-PA>.

Seright, R. S. 2003b. Washout of Cr(III)-Acetate-HPAM Gels from Fractures. Presented at the International Symposium on Oilfield Chemistry, Houston, 5–7 February. SPE-80200-MS. <http://dx.doi.org/10.2118/80200-MS>.

Seright, R. S., Lane, R. H., and Sydansk, R. D. 2003. A Strategy for Attacking Excess Water Production. *SPE Prod & Fac* **18** (3): 158–169. SPE-84966-PA. <http://dx.doi.org/10.2118/84966-PA>.

Seright, R. S., Liang, J. -T., Schrader, R. et al. 1998. *Improved Methods for Water Shutoff—Final Technical Progress Report*. US DOE Report No. DOE/PC/91008-14, US Department of Energy, Washington, D.C.

Sydansk, R. D. 1990. A Newly Developed Chromium (III) Gel Technology. *SPE Res Eng* **5** (3): 346–352. SPE-19308-PA. <http://dx.doi.org/10.2118/19308-PA>.

Sydansk, R. D. and Moore, P. E. 1992. Gel Conformance Treatments Increase Oil Production in Wyoming. *Oil Gas J* **90** (03).

Sydansk, R. D. and Southwell, G. P. 2000. More Than 12 Years' Experience with a Successful Conformance-Control Polymer-Gel Technology. *SPE Prod & Oper* **15** (4): 270–278. SPE-66558-PA. <http://dx.doi.org/10.2118/66558-PA>.

Tipura, L. 2008. *Wettability Characterization by NMR T₂ Measurements in Edwards Limestone*. MS thesis, University of Bergen, Bergen, Norway (March 2008).

- Willhite, G. P. and Pancake, R. E. 2008. Controlling Water Production Using Gelled Polymer Systems. *SPE Res Eval & Eng* **11** (3): 454–465. SPE-89464-PA. <http://dx.doi.org/10.2118/89464-PA>.
- Wilton, R. and Asghari, K. 2007. Improving Gel Performance in Fractures: Chromium Pre-Flush and Overload. *J Can Pet Technol* **46** (2): 33–39. <http://dx.doi.org/10.2118/07-02-04>.
- Witherspoon, P. A., Wang, J. S. Y., Iwai, K. et al. 1980. Validity of Cubic Law for Fluid Flow in a Deformable Rock Fracture. *Water Resour Res* **16** (6): 1016–1024. <http://dx.doi.org/10.1029/WR016i006p01016>.
- Zhang, H. and Bai, B. 2011. Preformed-Particle-Gel Transport Through Open Fractures and Its Effect on Water Flow. *SPE J.* **16** (2): 388–400. SPE-129908-PA. <http://dx.doi.org/10.2118/129908-PA>.
- Zou, B., McCool, C. S., Green, D. W. et al. 2000. Precipitation of Chromium Acetate Solutions. *SPE J.* **5** (3): 324–330. SPE-65703-PA. <http://dx.doi.org/10.2118/65703-PA>.

Bergit Brattekkås is a researcher at the National IOR Centre of Norway. Her research interests are enhanced oil recovery and flow mechanisms in mature oil reservoirs (e.g., increasing sweep efficiency by injection of polymer gels or foam). Brattekkås holds MSc and PhD degrees in reservoir physics from the University of Bergen.

Stina G. Pedersen is an engineer within Special Core Analysis in Statoil ASA. She holds an MSc degree in reservoir physics from the University of Bergen.

Hilde T. Nistov is a fluids engineer at Halliburton. She holds an MSc degree in reservoir physics from the University of Bergen.

Åsmund Haugen is a senior engineer within Special Core Analysis in Statoil ASA. Previously, he worked post-doctorate at the University of Bergen and as a visiting researcher at Rice University. Haugen's research interests are flow parameters; fluid flow in heterogeneous reservoirs; emphasizing wettability

effects; fracture-matrix interaction; spontaneous imbibition; fluid visualization; improved laboratory techniques; and enhanced-oil-recovery techniques, including foam, polymer gel, and CO₂ injection. He holds MSc and PhD degrees in reservoir physics from the University of Bergen.

Arne Graue is a professor of physics at the Department of Physics and Technology, University of Bergen, where he is head of the Petroleum and Process Technology Research Group. His scientific interest is within reservoir physics, emphasizing heterogeneous and fractured reservoirs, multiphase flow in porous media, in-situ fluid-saturation imaging, laboratory investigation of integrated enhanced-oil-recovery techniques, CO₂ sequestration, and gas hydrates. Graue has published more than 200 scientific publications and supervised more than 120 PhD-degree and MSc-degree students. He holds an MSc degree in experimental nuclear physics and a PhD degree in reservoir physics, both from the University of Bergen.

Jenn-Tai Liang is a professor in the Harold Vance Petroleum Engineering Department at Texas A&M University. Previously, he was a professor of petroleum engineering and director of the Tertiary Oil Recovery Program at the University of Kansas. Liang's research interests include the use of nanotechnology for water shutoff and conformance control, scale inhibition, wax and asphaltene inhibitions, and fracture-fluid cleanup. He has authored or coauthored more than 40 technical papers and holds seven patents. Liang holds a PhD degree in petroleum engineering from the University of Texas at Austin. He is a member of SPE.

Randall S. Seright is a senior engineer at the Petroleum Recovery Research Center of New Mexico Tech, where he has worked the past 27 years. He holds a PhD degree in chemical engineering from the University of Wisconsin at Madison and a BS degree in chemical engineering from Montana State University at Bozeman.